http://dx.doi.org/10.5012/bkcs.2011.32.11.4086

Identification of Two Eya2 Phosphatase Inhibitors from Virtual Screening with Docking Simulations

Hwangseo Park,[*] Keum Ran Yu,[†] and Seung Jun Kim[†,*]

Department of Bioscience and Biotechnology, Sejong University, Seoul 143-747, Korea
[*]E-mail: hspark@sejong.ac.kr
[†] Medical Proteomics Research Center, Korea Research Institute of Bioscience and Biotechnology, Daejeon 305-600, Korea
[*]E-mail: ksj@kribb.re.kr
Received August 30, 2011, Accepted September 15, 2011

Key Words : Eya2 phosphatase, Virtual screening, Inhibitor, Docking, Cancer

Protein tyrosine phosphatases (PTPs) serve as a hallmark in the signal transductions through the hydrolysis of the phosphorylated tyrosine residue on various protein substrates. Most of PTPs share common structural features and use a cysteine residue as the nucleophile in their catalytic reactions involving a thiol-phosphate intermediate.[1] Eyes absent PTPs (Eya's) differ from the other PTPs in that they use an aspartate residue and a metal ion as the nucleophile and the Lewis acid catalyst, respectively, in the catalytic reactions.[2] Due to the role of a determinant for the life and death fate in response to genotoxic stress, Eya's may be involved in a variety of cancers. For example, Eyes absent homologue 2 (Eya2) was shown to be up-regulated in ovarian cancer[3] and lung adenocarcinoma.[4] The inhibition of Eya4 reduced the tumorigenic properties of the malignant peripheral nerve sheath tumor *in vitro* and resulted in cell death *in vivo*.[5] Very recently, it was also shown that the tyrosine phosphatase activity of Eya should be responsible for the migration, invasion, and transformation of tumor cells.[6] It is thus apparent that Eya's play a critical role in tumorigenesis, and therefore the inhibition of their catalytic activity can be a promising therapeutic strategy for the treatment of cancers.

Recently the X-ray crystal structure of Eya2 was reported in the ligand-bound form,[7] which provided a good opportunity to discover the inhibitors that can be developed into new cancer drugs. Nonetheless, no small-molecule inhibitor of Eya's has been reported so far. In the present work, we identify novel classes of Eya2 inhibitors by means of the structure-based virtual screening with docking simulations and *in vitro* enzyme assay. Thus, we report the first example for the discovery of Eya2 inhibitors. It will be shown that docking simulations can be a useful tool for enriching the chemical library used in screening assays with molecules that are likely to have the desired biological activities as well as for elucidating the activities of the identified inhibitors.

Of the 85,000 compounds subject to the virtual screening with docking simulations, 100 top-scored compounds were selected as virtual hits. 87 of them were available from the compound supplier and were tested for inhibitory activity against Eya2 phosphatase by *in vitro* enzyme assay. This inhibition assay was performed in duplicates at all concentrations of the inhibitors and the average values were used as data points. As a result, we identified two compounds that inhibited the catalytic activity of Eya2 by more than 50% at the concentration of 25 μM. The chemical structures and the inhibitory activities of the newly identified inhibitors are shown in Figure 1 and Table 1, respectively. To the best of our knowledge, neither of these compounds has been reported as a phosphatase inhibitor so far. We note that the terminal ester moiety of **1** and one of the methoxy groups attached to the terminal phenyl ring of **2** serve as a ligand for the active-site Mg^{2+} ion. Although the inhibitory activities of **1** and **2** are moderate with IC_{50} values ranging from 10 to 25 μM, they are expected to have good physicochemical properties as a drug candidate because they were screened based on Lipinski's "Rule of Five". Therefore, both inhibitors deserve considerations for further development by structure-activity relationship (SAR) studies to improve the anticancer activities.

To obtain some energetic and structural insight into the inhibitory mechanisms by the two identified inhibitors of Eya2, their binding modes in the active site were investigated using the AutoDock program. The calculated binding mode of **1** in the active site of Eya2 is shown in Figure 2. In

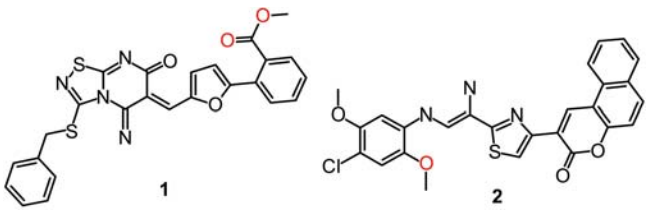

Figure 1. Chemical structures of the newly identified Eya2 phosphatase inhibitors. The atoms coordinated to the Mg^{2+} ion are indicated in red.

Table 1. Inhibitory activities of **1** and **2** and against Eya2 phosphatase

Compound	IC_{50} (μM)
1	13.7 ± 0.4
2	24.1 ± 1.7

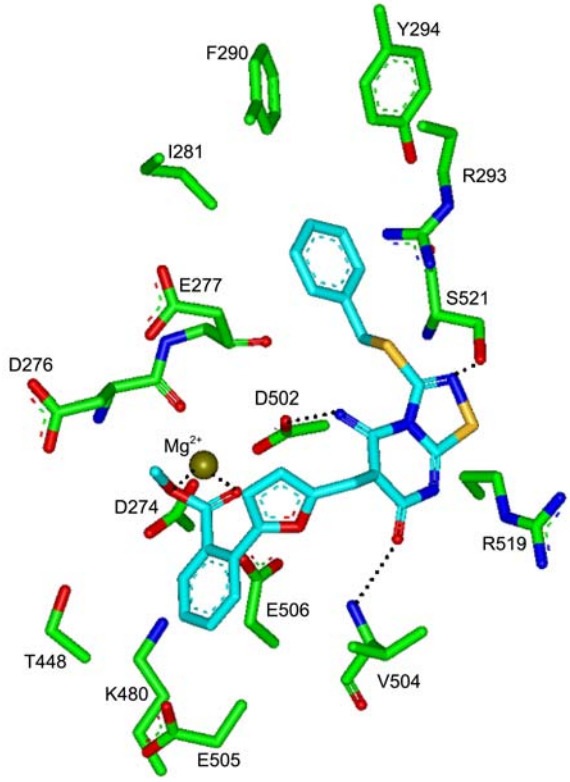

Figure 2. Binding mode of **1** in the active site of Eya2 phosphatase. Carbon atoms of the protein and the ligand are indicated in green and cyan, respectively. Each dotted line indicates a hydrogen bond or a coordination to the central Mg^{2+} ion.

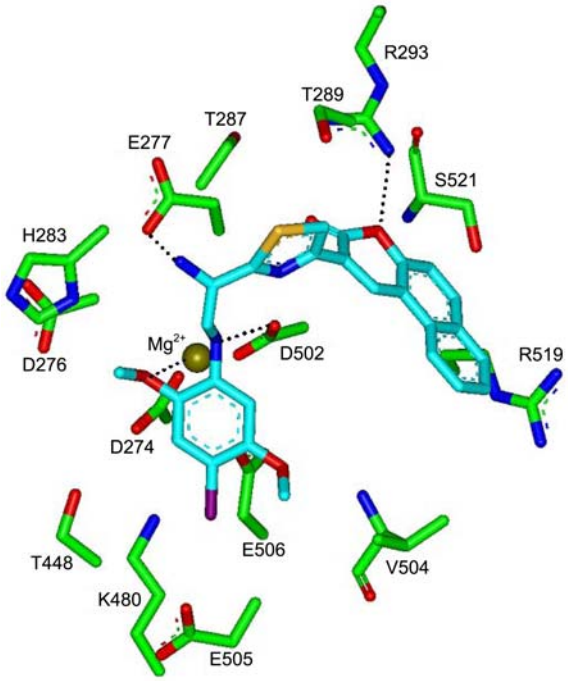

Figure 3. Binding mode of **2** in the active site of Eya2 phosphatase. Carbon atoms of the protein and the ligand are indicated in green and cyan, respectively. Each dotted line indicates a hydrogen bond or a coordination to the central Mg^{2+} ion.

this calculated Eya2-**1** complex, the two oxygen atoms of the terminal ester moiety are coordinated to the central Mg^{2+} ion with the associated O···Mg distances of 2.04 and 2.18 Å for sp^2 and sp^3 oxygens, respectively. The carbonyl oxygen and iminyl nitrogen attached to the central six-membered ring receives and donates a hydrogen bond from the backbone amidic group of Val504 and to the side-chain carboxylate moiety of Asp502, respectively. Judging from the proximity to the Mg^{2+} ion complex, these hydrogen bonds seem to play a significant role in maintaining the coordination of the neighboring ester group to the Mg^{2+} ion as well as in stabilizing **1** in the active site of Eya2. An additional affinity-enhancing hydrogen bond is also established between the nitrogen atom on the thiadiazole ring of **1** and the side-chain hydroxy moiety of Ser521. The inhibitor **1** can be further stabilized in the active site by establishing the hydrophobic interactions between its aromatic rings and the nonpolar residues including Ile281, Phe290, Tyr294, and Val504. On the basis of these structural features, it can be argued that **1** should be capable of impairing the enzymatic activity of Eya2 by binding in the active site through the simultaneous establishment of the multiple hydrogen bonds and hydrophobic interactions in addition to the chelation of the Mg^{2+} ion.

Figure 3 shows the most probable binding mode of **2** in the active site of Eya2 obtained from docking simulations. The binding mode of **2** differs from that of **1** in that only one oxygen atom at the terminal methoxy group is coordinated to the central Mg^{2+} ion. The anilinic and the amine groups that reside between phenyl and thiazole rings donate the hydrogen bonds to the side-chain carboxylate groups of Asp502 and Glu277, respectively. An oxygen atom on pyra-2-one ring of **2** stays at a distance of 2.71 Å from the side-chain guanidium ion of Arg293, which indicates the involvement of an additional hydrogen bond in the formation of Eya2-**2** complex. Hydrophobic interactions in Eya2-**2** complex seem to be established in a weaker form than those in Eya2-**1** complex because only one nonpolar residue (Val504) is observed at the interface of the former. Because the number of the hydrogen bonds is the same in Eya2-**1** and Eya2-**2** complexes, the lower inhibitory activity of **2** than **1** can be attributed to the decrease in the number of coordination bonds to the central Mg^{2+} ion and the weakening of hydrophobic interactions in the active site.

In summary, we have identified two new novel inhibitors of Eya2 phosphatase by means of the structure-based virtual screening with docking simulations. These inhibitors exhibit a significant potency with IC_{50} values of 13.7 and 24.1 μM and have a proper ligand groups to be coordinated to the active-site Mg^{2+} ion. Considering the novelty and the potency, these two Eya2 inhibitors deserve consideration for further development by SAR studies to optimize the anticancer activity. Detailed binding mode analyses with docking simulation indicate that besides the coordination to the central Mg^{2+} ion, the inhibitors can be stabilized in the active site by the simultaneous establishment of the multiple hydrogen bonds and van der Waals contacts.

Experimental Section

Virtual Screening of Eya2 Phosphatase Inhibitors. The X-ray crystal structure of Eya2 phosphatase in complex with a substrate analogue (PDB code: 3HB0)[7] was selected as the receptor model in the virtual screening with docking simulations. After removing the ligand and solvent molecules, hydrogen atoms were added to each protein atom. A special attention was paid to assign the protonation states of the ionizable Asp, Glu, His, and Lys residues. The side chains of Asp and Glu residues were assumed to be neutral if one of their carboxylate oxygens pointed toward a hydrogen-bond accepting group including the backbone aminocarbonyl oxygen at a distance within 3.5 Å, a generally accepted distance limit for a hydrogen bond of moderate strength. Similarly, the lysine side chains were assumed to be protonated unless the NZ atom was in proximity to a hydrogen-bond donating group. The same procedure was also applied to determine the protonation states of ND and NE atoms in His residues.

The docking library for Eya2 phosphatase comprising about 85,000 compounds was constructed from the latest version of the chemical database distributed by Interbioscreen (http://www.ibscreen.com) containing approximately 30,000 natural and 320,000 synthetic compounds. The selection was based on the drug-like filters that adopt only the compounds with physicochemical properties of potential drug candidates[9] and without reactive functional group(s). All of the compounds included in the docking library were then subjected to the CORINA program to generate their three-dimensional atomic coordinates, followed by the assignment of Gasteiger-Marsilli atomic charges.[10] We used the AutoDock program[11] in the virtual screening of Eya2 phosphatase inhibitors because the outperformance of its scoring function over those of the others had been shown in several target proteins.[12,13] AMBER force field parameters were assigned for calculating the van der Waals interactions and the internal energy of a ligand as implemented in the AutoDock program.

***In vitro* Enzyme Inhibition Assay.** Enzyme assays were performed using 6,8-difluoro-4-methylumbelliferyl phosphate (DIFMUP) as a substrate at 25 °C and pH 6.5 in the presence or absence of an inhibitor in the reaction vessel including 20 mM MES, 150 mM NaCl, 5 mM DTT, and 2 mM $MgCl_2$. After adding purified Eya2 (50 nM) and DIFMUP (20 μM), the reactions were allowed to proceed for 90 min at room temperature, and were stopped by adding sodium orthovanadate (1 mM). The fluorescence intensity was measured (355 nm excitation and 460 nm emission) using a plate reader. IC_{50} values were determined directly from the regression curves constructed using the tested inhibitors. This procedure was repeated in duplicate for all of the putative inhibitors to obtain their average IC_{50} values.

Acknowledgments. This work was supported by Grant No. K11061 from the Korea Institute of Oriental Medicine (KIOM), and by Grant No. 2011-0018011 from National Research Foundation (NRF) of Korea government.

References

1. Alonso, A.; Sasin, J.; Bottini, N.; Friedberg, I.; Friedberg, I.; Osterman, A.; Godzik, A.; Hunter, T.; Dixon, J.; Mustelin, T. *Cell* **2004**, *117*, 699.
2. Rayapureddi, J. P.; Kattamuri, C.; Steinmetz, B. D.; Frankfort, B. J.; Ostrin, E. J.; Mardon, G.; Hegde, R. S. *Nature* **2003**, *426*, 295.
3. Zhang, L.; Yang, N.; Huang, J.; Buckanovich, R. J.; Liang, S.; Barchetti, A.; Vezzani, C.; O'Brien-Jenkins, A.; Wang, J.; Ward, M. R.; Courreges, M. C.; Fracchioli, S.; Medina, A.; Katsaros, D.; Weber, B. L.; Coukos, G. *Cancer Res.* **2005**, *65*, 925.
4. Guo, J.; Liang, C.; Ding, L.; Zhou, N.; Ye, Q. *Chin. Ger. J. Clin. Oncol.* **2009**, *8*, 681.
5. Miller, S. J.; Lan, Z. D.; Hardiman, A.; Wu, J.; Kordich, J. J.; Patmore, D. M.; Hegde, R. S.; Cripe, T. P.; Cancelas, J. A.; Collins, M. H.; Ratner, N. *Oncogene* **2010**, *29*, 368.
6. Pandey, R. N.; Rani, R.; Yeo, E.-J.; Spencer, M.; Hu, S.; Lang, R. A.; Hegde, R. S. *Oncogene* **2010**, *29*, 2893.
7. Jung, S.-K.; Jeong, D. G.; Chung, S. J.; Kim, J. H.; Park, B. C.; Tonks, N. K.; Ryu, S. E.; Kim, S. J. *FASEB J.* **2010**, *24*, 560.
8. Lipinski, C. A.; Lombardo, F.; Dominy, B. W.; Feeney, P. J. *Adv. Drug Delivery Rev.* **1997**, *23*, 3.
9. Gasteiger, J.; Marsili, M. *Tetrahedron* **1980**, *36*, 3219.
10. Morris, G. M.; Goodsell, D. S.; Halliday, R. S.; Huey, R.; Hart, W. E.; Belew, R. K.; Olson, A. J. *J. Comput. Chem.* **1998**, *19*, 1639.
11. Park, J.-H.; Ko, S.; Park, H. *Bull. Kor. Chem. Soc.* **2008**, *29*, 921.
12. Lee, W.; Park, H.; Lee, S. *Bull. Kor. Chem. Soc.* **2008**, *29*, 363.